Native Enzyme Classical Simulation

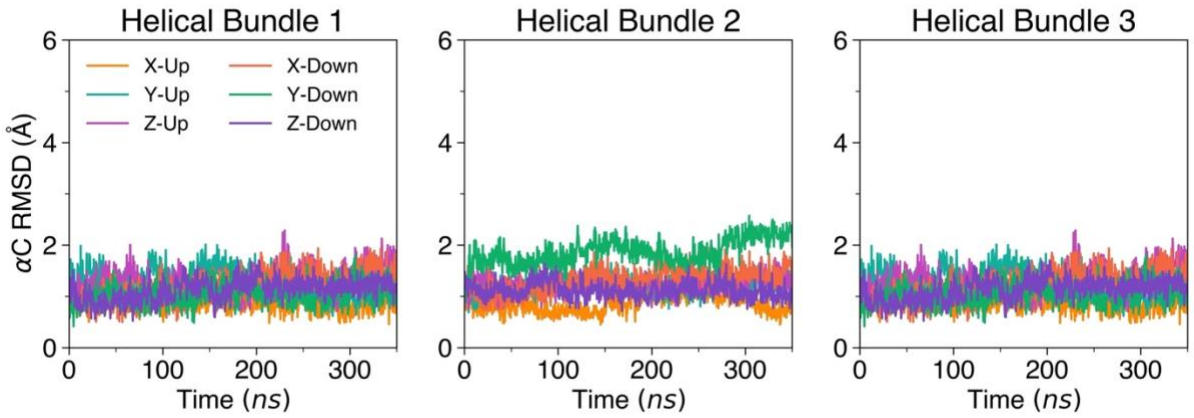

Figure S1: The α-carbon RMSD for all atoms included in the helical bundles which define enzyme orientation relative to the interface are evaluated to confirm the stability of the CV in the events of enzyme rotation and lid domain opening.

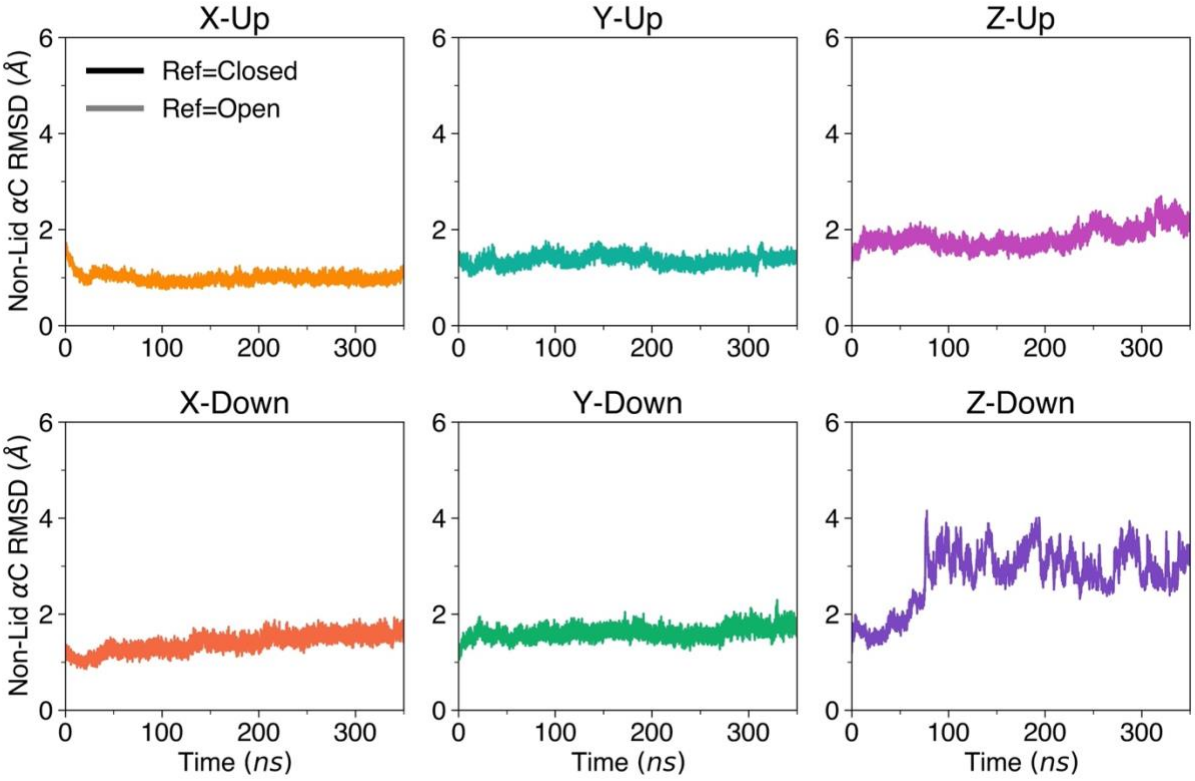

Figure S2: Non-lid α-carbon RMSD is evaluated with reference to the closed lid crystal structure (pdb: *1TRH*) to verify the stability of the enzyme during rotation and lid opening. Elevated values above 2 Å for trial Z-Down are attributable to the flexibility of the enzyme C-terminal tail.

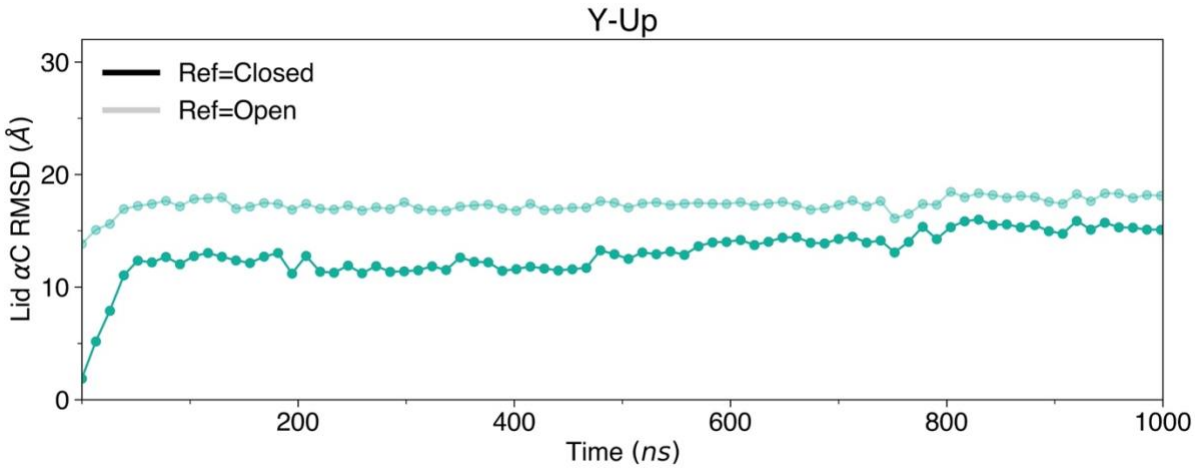

Figure S3: Lid α-carbon RMSD is evaluated with reference to the closed lid crystal structure (pdb: *1TRH*) out to 1 microsecond to verify the stability of the uniquely observed lid state.

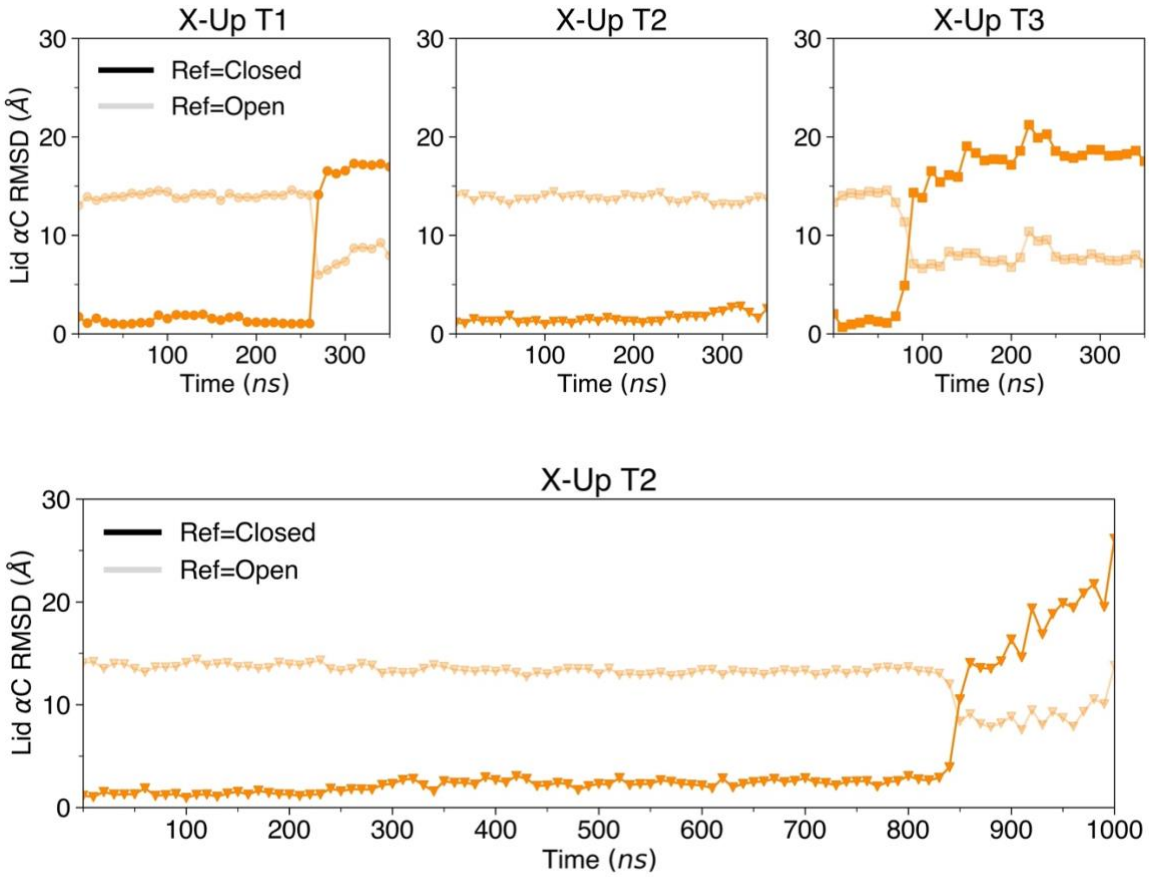

Figure S4: Lid α-carbon RMSD is evaluated with reference to the closed lid crystal structure (pdb: *1TRH*) for all trials of X-Up. X-Up trial 2 is extended out to 1 microsecond to demonstrate lid opening that occurs at approximately 800 ns.

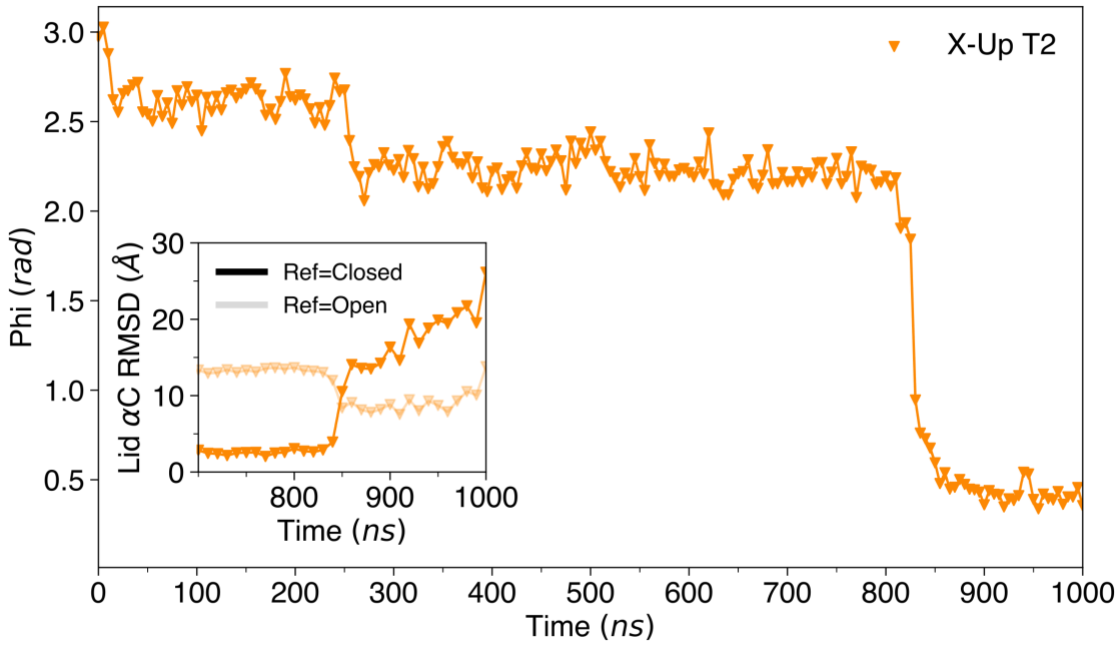

Figure S5: The orientation of the enzyme relative to the interface is evaluated based on collective variable ϕ of the course of the 1 microsecond simulation for the extended run of X-Up trial 2. Rapid rotation is observed towards a value of $\phi \approx 0.4$ rad at approximately 800 ns. This rotation is shown to coincide with lid domain rearrangement as evidence by increasing lid α-carbon RMSD reference to the closed lid crystal structure (pdb: *1TRH*) and decreasing lid α-carbon RMSD reference to the open lid crystal structure (pdb: *1CRL*)

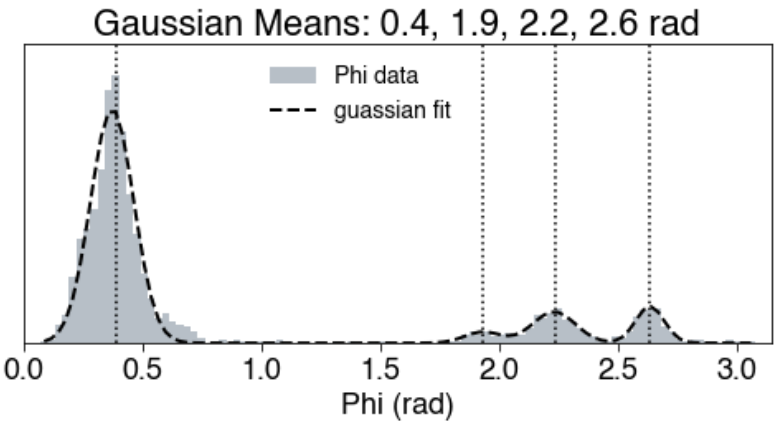

Figure S6: All ϕ data within the first 350 ns of simulations was fit to a sum of four gaussians, resulting in 4 mean values representing the centers of each distribution ($\phi = 0.4,1.9,2.2,2.6$)

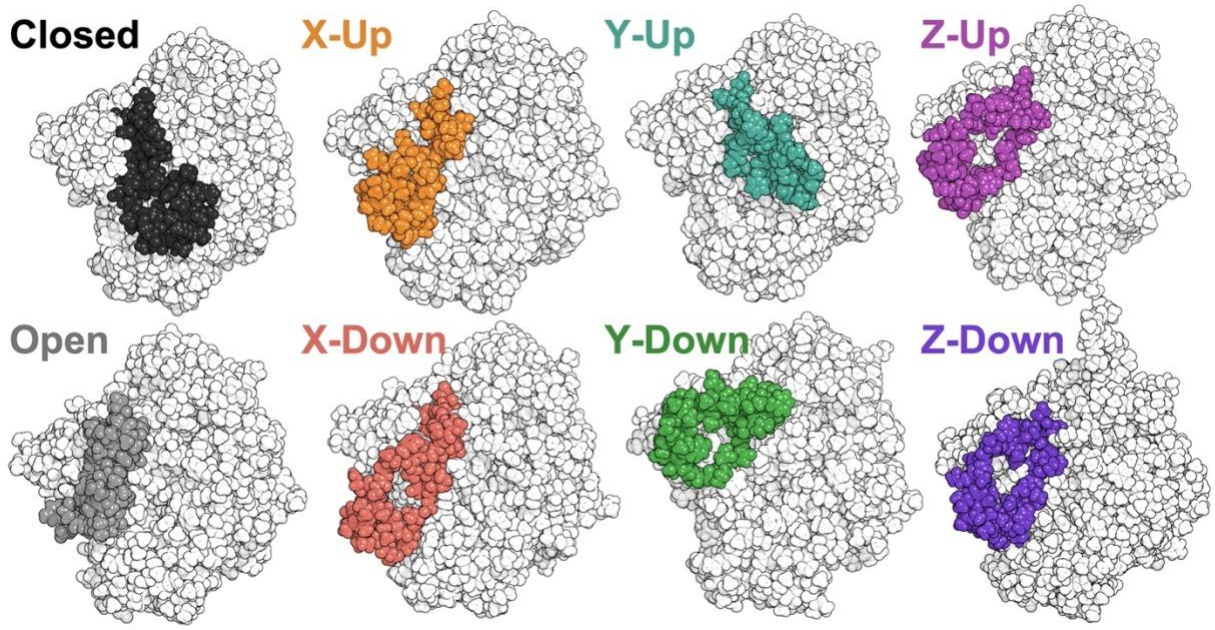

Figure S7: Native CRL is shown in the closed (black) and open (gray) crystal structures alongside trial 1 for each initial orientation sampled at 350 ns. Lid domains (residues 60 to 97) are highlighted by differing colors in each trial.

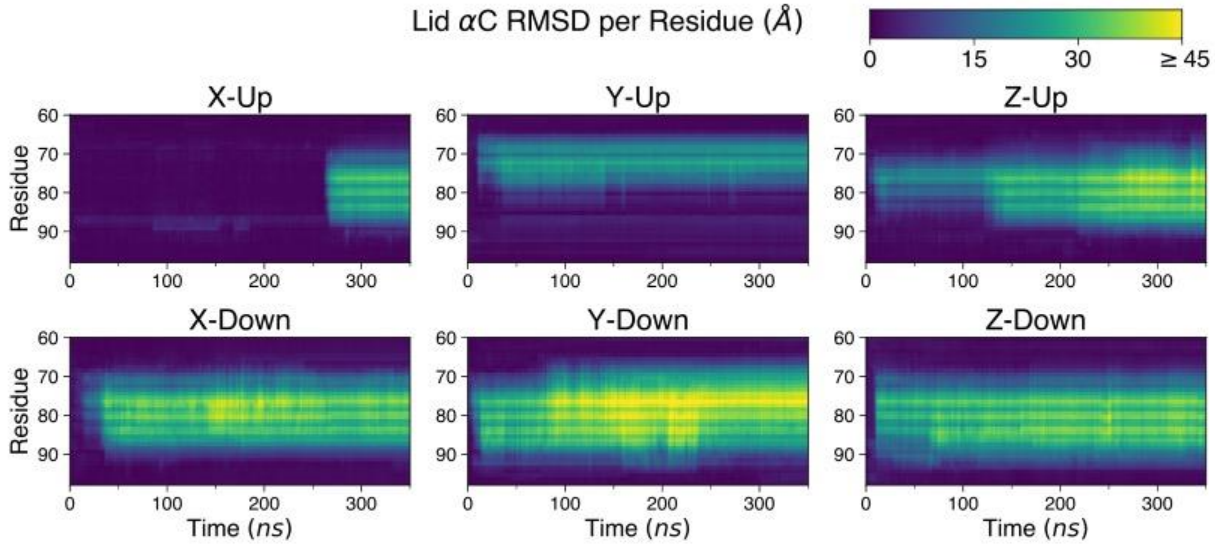

Figure S8: α-carbon RMSD was evaluated per residue in the lid domain (residues 60-97) for the first 350 ns of each trial. Greatest flexibility in the lid domain is observed for residues at the center of the flap (residues 70-87). Y-Up demonstrates a unique fold in which residues 85-97 demonstrate negligible rearrangement.

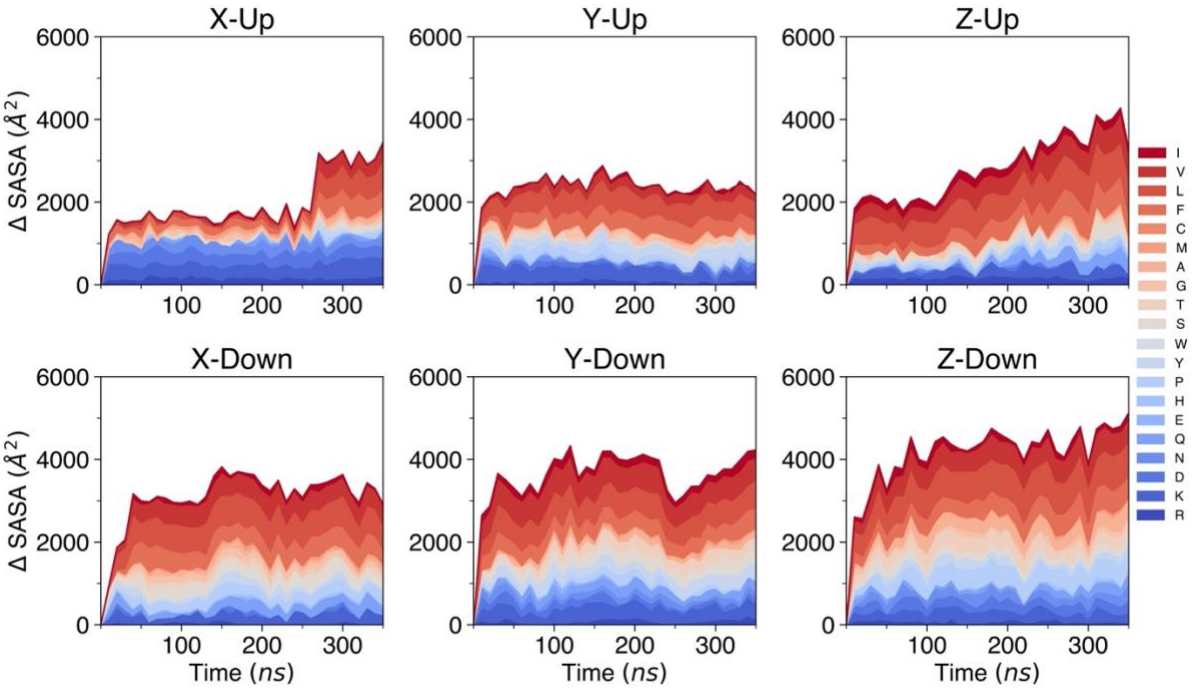

Figure S9: *ΔSASA* is measured relative to the start frame and grouped by amino acid residue name. Residues are sorted according to theoretical hydropathy index[1] and colored from least hydrophobic (blue) to most hydrophobic (red).

Native Enzyme Biased Simulation

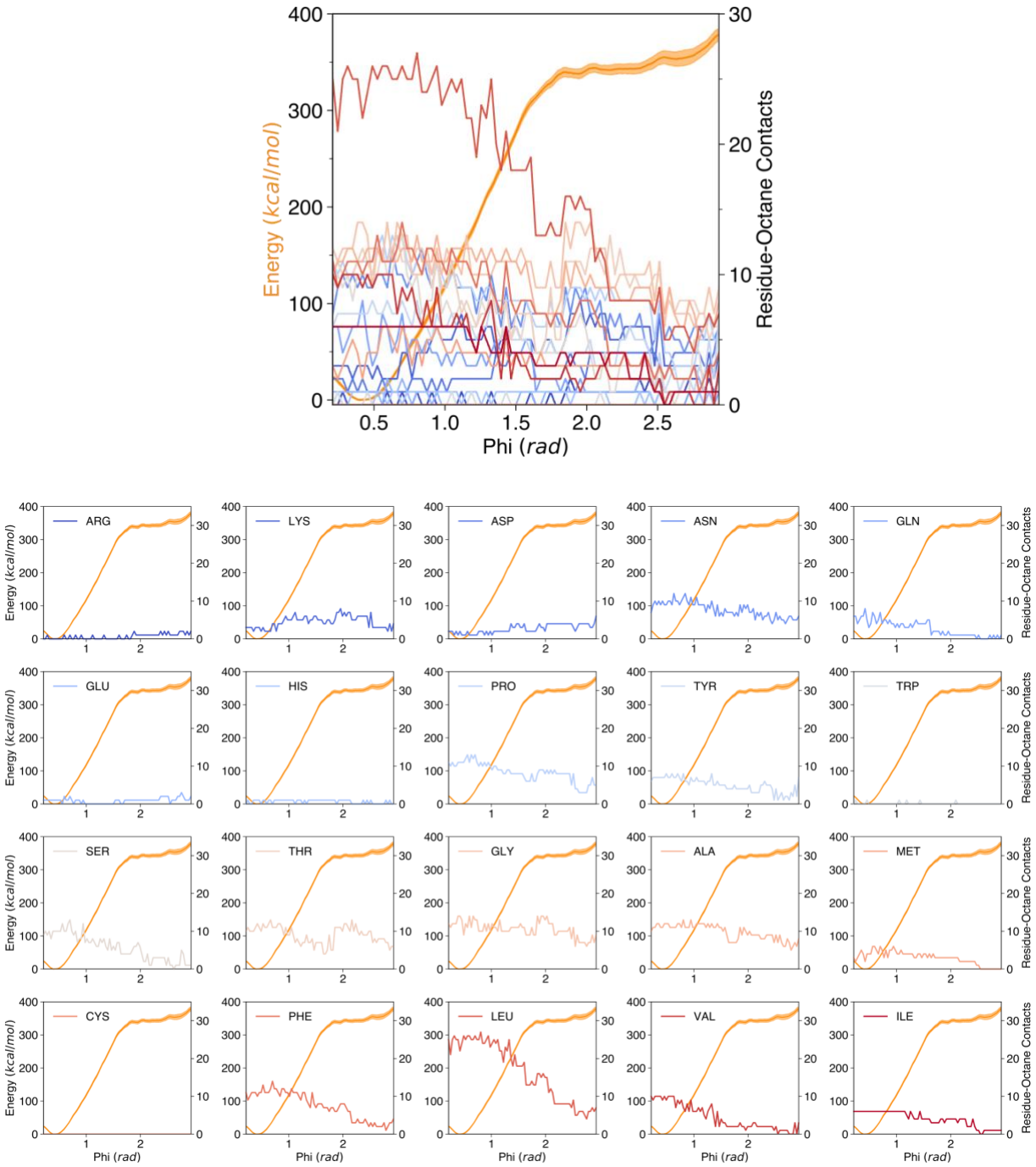

Figure S10: Enzyme-octane phase contacts are evaluated for 20 residue types and sorted and colored based on increasing theoretical hydrophobicity[1] (blue to red). Residue contact values are averaged for each window in the range of $\phi = 0.35$ to $\phi = 2.97$ rad. All contact counts are plotting alongside the evaluated free energy (orange) at the corresponding values of ϕ, leaving up to 40 ns to equilibration for interfacial windows.

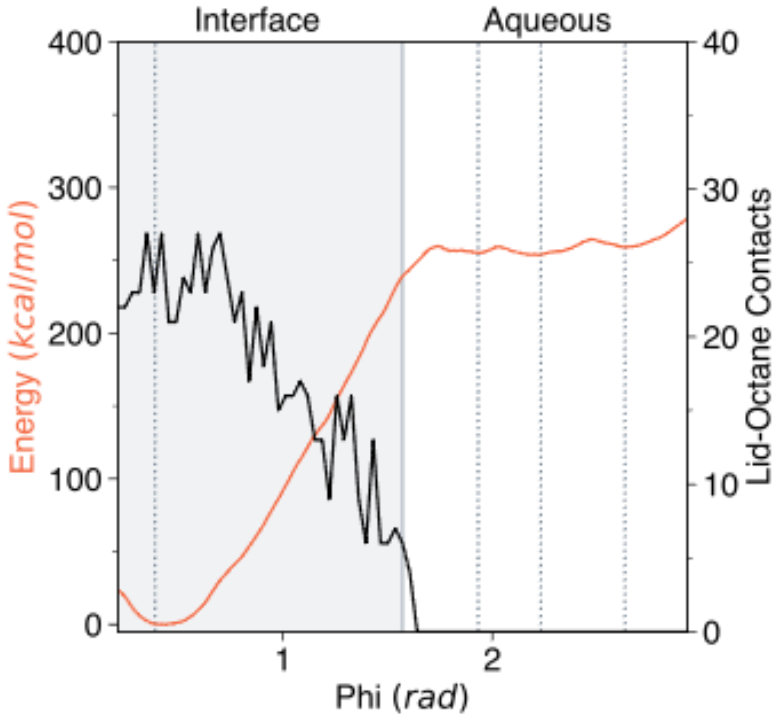

Figure S11: The free energy of rotation (red) for enzyme CRL at the oil-water interface was evaluated over a range $\phi = 0.35$ to $\phi = 2.97$ rad. Initially, 5 ns of simulation were included for all frames. Minima predicted from unbiased simulations are marked by dotted lines at $\phi = 0.4,1.9,2.2,2.6$ rad. Two regions of the simulation, interface and aqueous, are differentiated by the shaded and non-shaded regions, respectively. Interfacial windows exhibit contact (within 4 Å) between the lid domain and the octane phase and in turn demonstrate interfacial activation and lid domain rearrangement. The separation between these two states is highlighted by the average number of lid-octane contacts in each window (black).

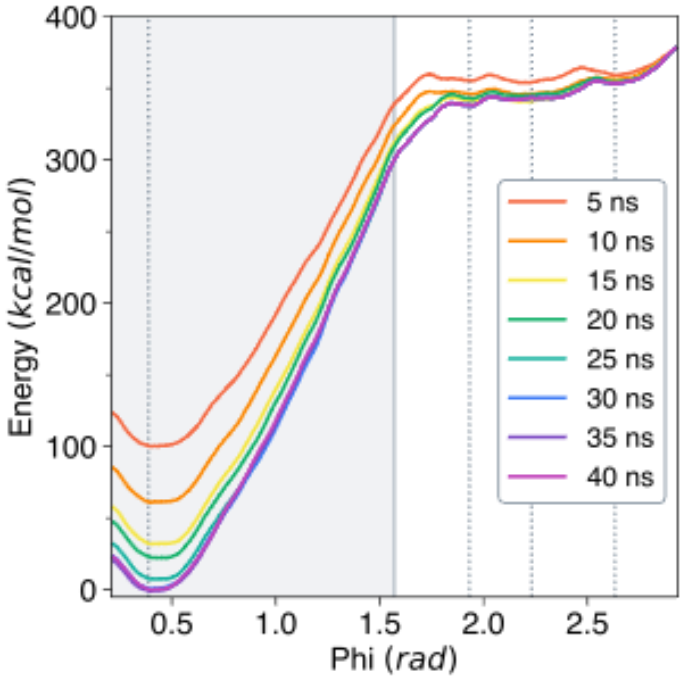

Figure S12: The free energy of rotation for enzyme CRL at the oil-water interface was evaluated over a range $\phi = 0.35$ to $\phi = 2.97$ rad for varying durations of equilibration starting at 5 ns and increasing up to 40 ns. Regardless of equilibration time, all production frames used for evaluating free energy include 10 ns of simulation time. Free energies are aligned at the global maximum value observed at $\phi = 2.97$.

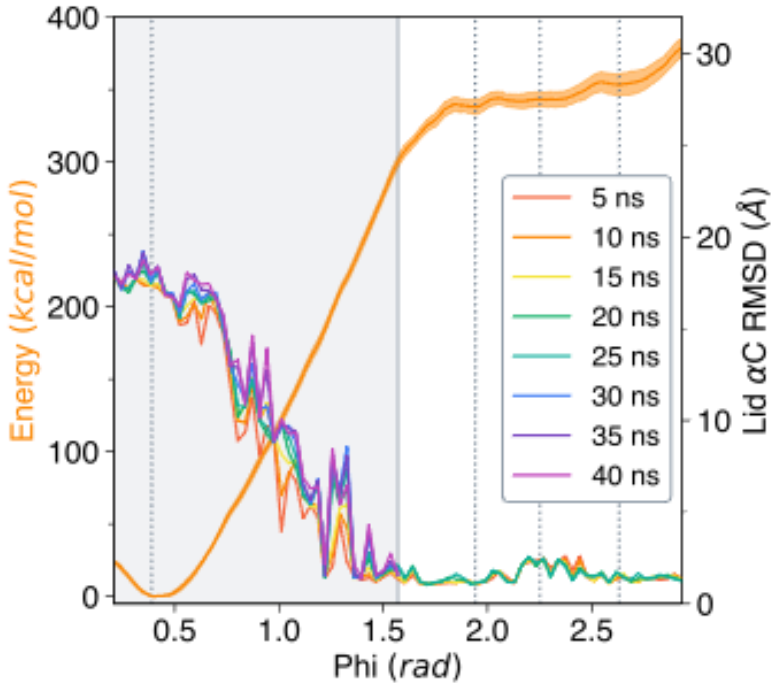

Figure S13: The free energy The free energy of rotation for enzyme CRL at the oil-water interface was evaluated over a range $\phi = 0.35$ to $\phi = 2.97$ rad for an equilibration time of 40 ns for interfacial windows (orange). Uncertainty was evaluated based on Monte Carlo bootstrapping in WHAM with a decorrelation time of 300 time steps (1.2 ps). This is presented alongside lid α-carbon RMSD referenced to the closed lid state (pdb: *1TRH*) at corresponding values of ϕ for each equilibration period considered. RMSD values represent maximum values among production frames for each window with all production frames corresponding to 10 ns of simulation time regardless of equilibration period.

Mutant Enzyme Unbiased Simulation

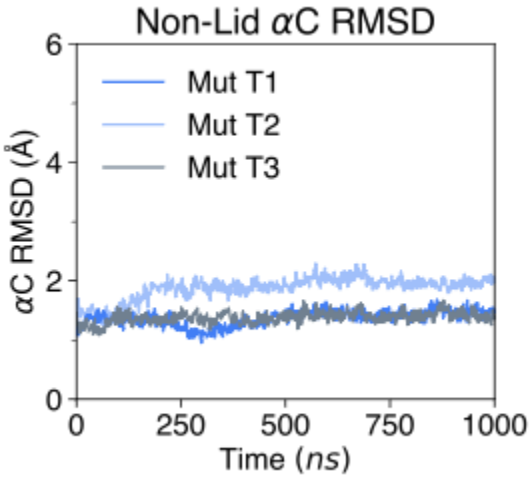

Figure S14: Non-lid α-carbon RMSD is evaluated with reference to the closed lid crystal structure (pdb: *1TRH*) to verify the stability of the enzyme during rotation.

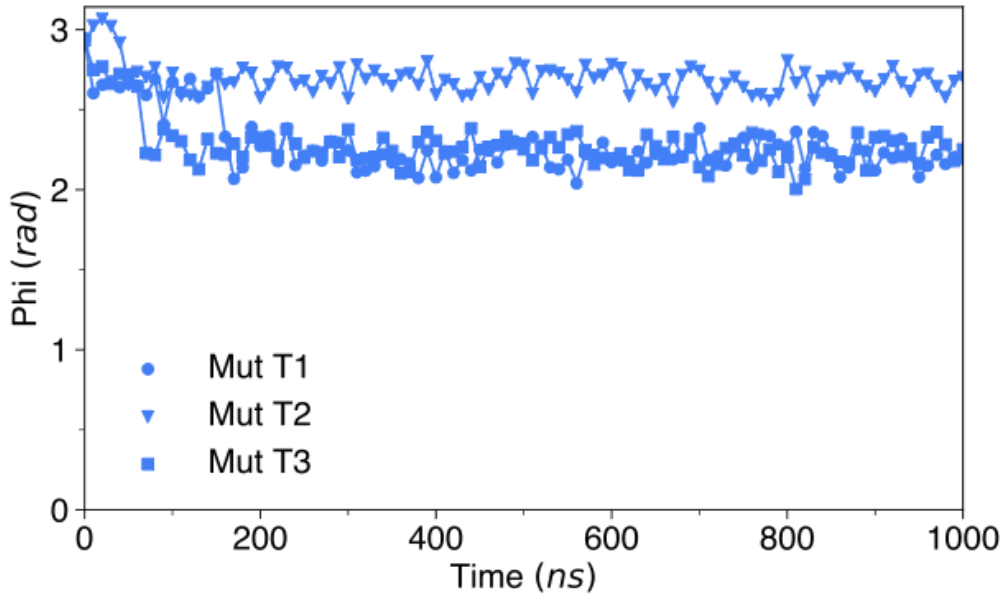

Figure S15: The time series data monitors the value of ϕ (CV defining enzyme orientation relative to the interface) for three trials of the mutant enzyme beginning from the X-Up orientation relative to the interface with variable solvent packing. Trials are differentiated by marker shape. Data is plotted every 5 ns for clarity. Rotation beyond $\phi \approx 2.2$ is not observed for any trial.

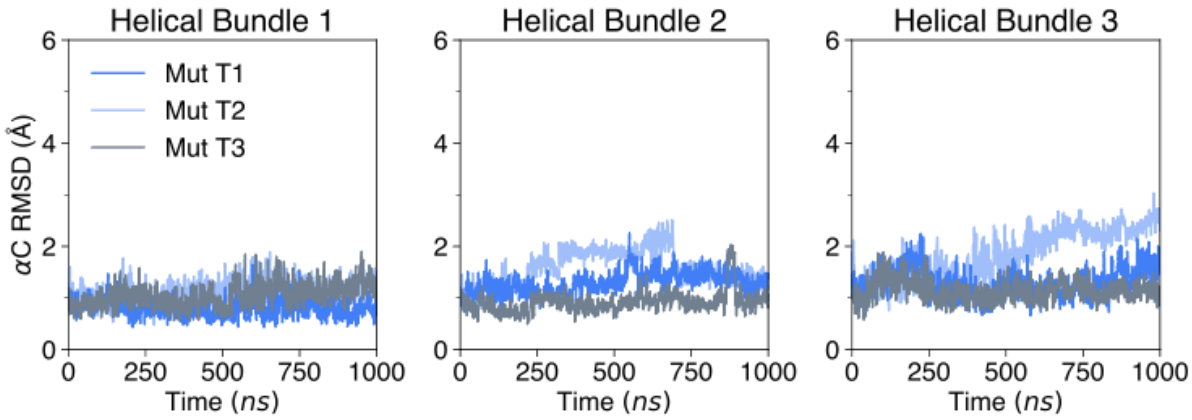

Figure S16: The α-carbon RMSD for all atoms included in the helical bundles which define enzyme orientation relative to the interface are evaluated to confirm the stability of the CV in the events of enzyme rotation.

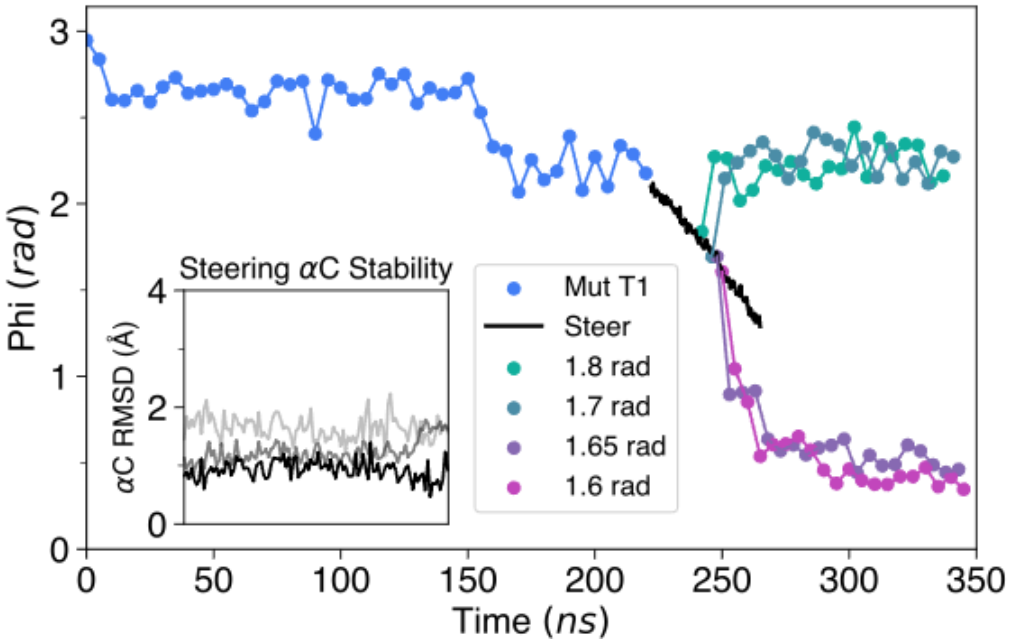

Figure S17: Unbiased simulation for mutant enzyme trial 1 is plotted (blue) out to approximately 200 ns. Steering was performed to direct the enzyme between values of ϕ spanning 2.1 to 1.3 rad. Frames for steering were extracted at values of phi corresponding to 1.8, 1.7 1.65, and 1.6 rad and run unbiased. While trajectories beginning from $\phi = 1.7,1.8$ demonstrate return to $\phi \approx 2.2$ radians, those beginning from $\phi = 1.6,1.65$ exhibit continued rotation to $\phi \approx 0.4$ rad. The stability of the enzyme backbone during steering is verified by negligible rearrangement in α-carbon RMSD referenced to the closed lid state (pdb: *TRH*).

Mutant Enzyme Biased Simulation

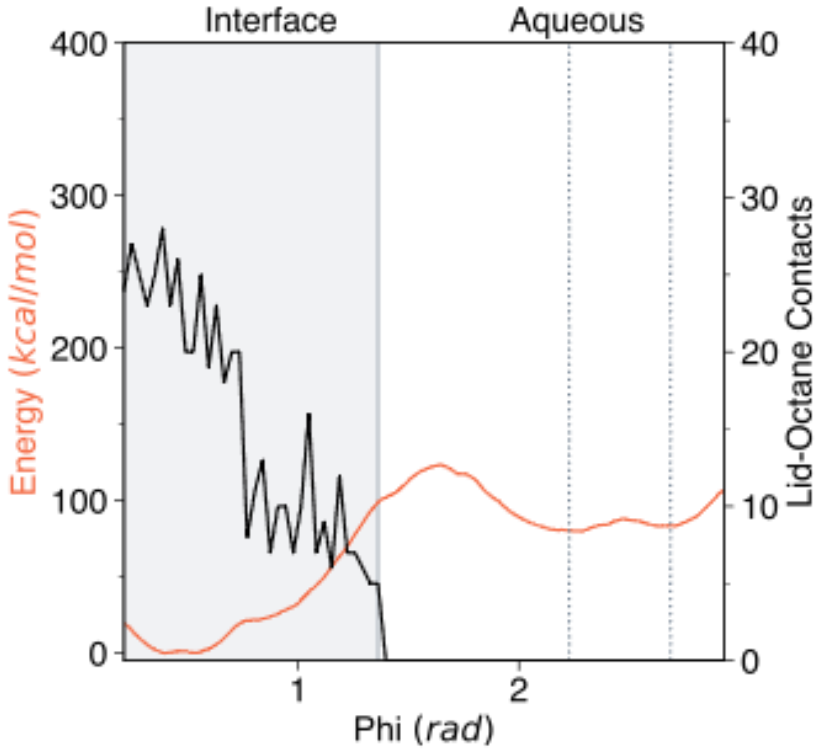

Figure S18: The free energy of rotation (red) for mutant CRL at the oil-water interface was evaluated over a range $\phi = 0.35$ to $\phi = 2.97$ rad. Initially, 5 ns of simulation were included for all frames. Minima predicted from unbiased simulations are marked by dotted lines at $\phi = 2.3, 2.6$ rad. Two regions of the simulation, interface and aqueous, are differentiated by the shaded and non-shaded regions, respectively. Interfacial windows exhibit contact (within 4 Å) between the lid domain and the octane phase and in turn demonstrate interfacial activation and lid domain rearrangement. The separation between these two states is highlighted by the average number of lid-octane contacts in each window (black).

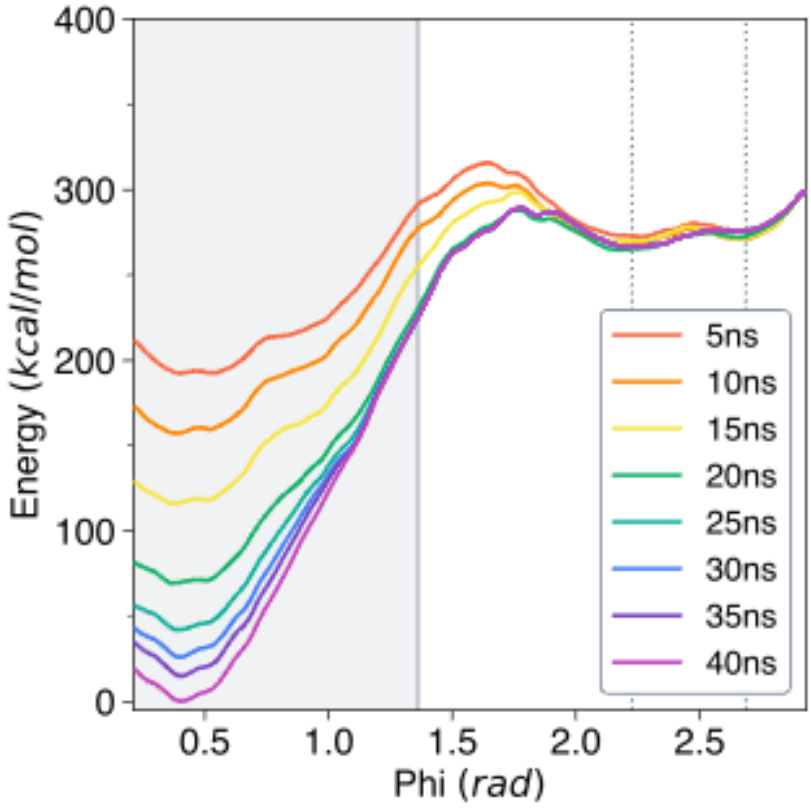

Figure S19: The free energy of rotation for mutant CRL at the oil-water interface was evaluated over a range $\phi = 0.35$ to $\phi = 2.97$ rad for varying durations of equilibration starting at 5 ns and increasing up to 40 ns. Regardless of equilibration time, all production frames used for evaluating free energy include 10 ns of simulation time. Free energies are aligned at $\phi = 2.97$.

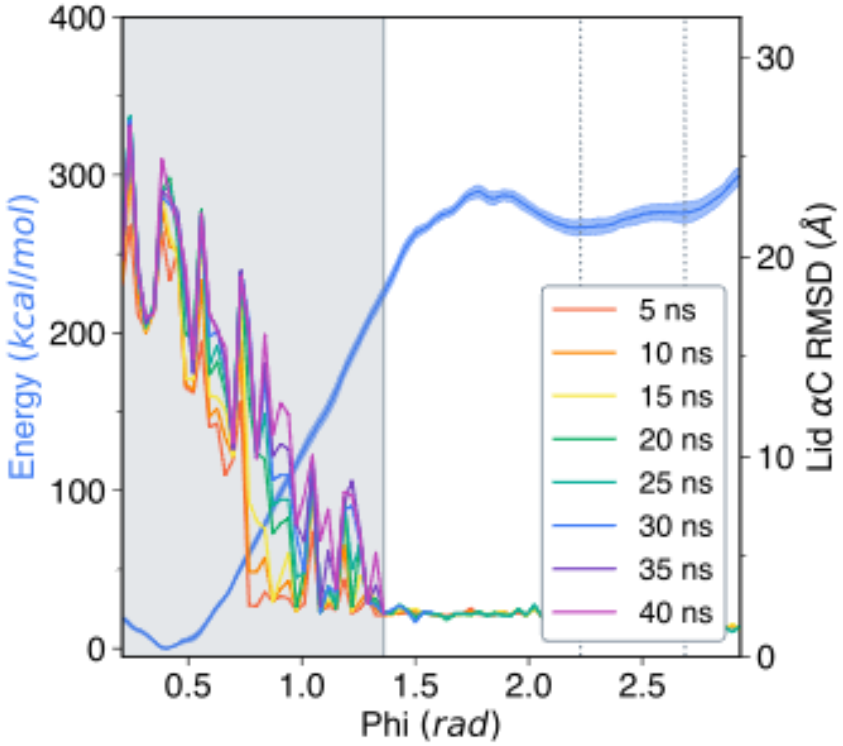

Figure S20: The free energy of rotation for mutant CRL at the oil-water interface was evaluated over a range $\phi = 0.35$ to $\phi = 2.97$ rad for an equilibration time of 40 ns for interfacial windows (blue). Uncertainty was evaluated based on Monte Carlo bootstrapping in WHAM with a decorrelation time of 300 time steps (1.2 ps). This is presented alongside lid α-carbon RMSD referenced to the closed lid state (pdb: *1TRH*) at corresponding values of ϕ for each equilibration period considered. RMSD values represent maximum values among production frames for each window with all production frames corresponding to 10 ns of simulation time regardless of equilibration period.

Individual Amino Acid Study

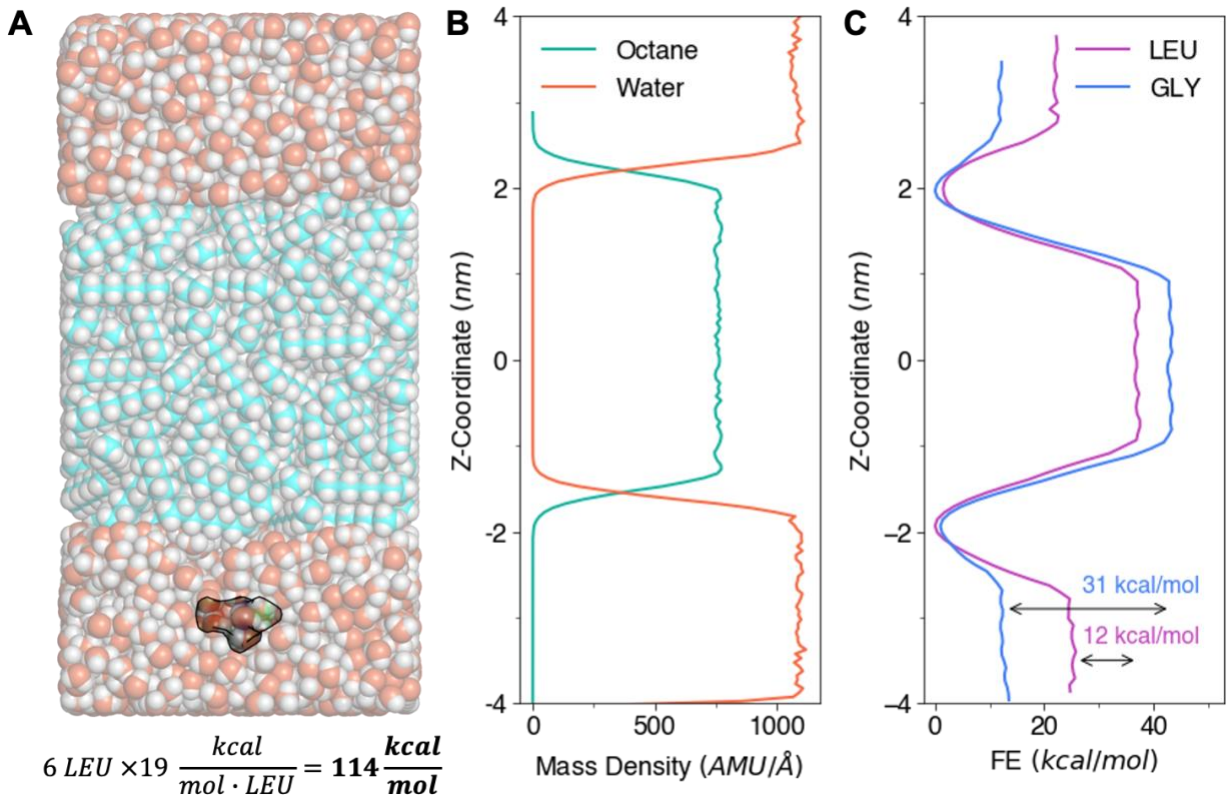

$$6\ LEU \times 19\ \frac{kcal}{mol \cdot LEU} = \mathbf{114}\frac{\boldsymbol{kcal}}{\boldsymbol{mol}}$$

Figure S21: (a) Monomers of LEU and GLY with ACE/NME caps were pulled through two water-octane interfaces by steering to generate windows spaced every 0.5 Å for Umbrella Sampling with a restraint constant of $500\ \frac{kcal}{mol \cdot rad}$. (b) The mass density of octane and water molecules averaged for all frames in each window demonstrate good preservation of the interface in all windows. (c) Free energy profiles for LEU (pink) and GLY (blue) are plotted as a function of the z-coordinate along through the two oil-water interfaces. The ΔG corresponding to a transition between full immersion in the water phase and octane phase is shown to be 12 $\frac{kcal}{mol}$ for LEU and 31 $\frac{kcal}{mol}$ for GLY, yielding a $\Delta\Delta G$ of 19 $\frac{kcal}{mol}$.

References

1. Kyte, J.; Doolittle, R. F. A Simple Method for Displaying the Hydropathic Character of a Protein. *J. Mol. Biol.* **1982**, *157* (1), 105–132. https://doi.org/10.1016/0022-2836(82)90515-0.